BMC Biotechnology

RESEARCH Open Access

# Synergistic effect of zinc oxide-cinnamic acid nanoparticles for wound healing management: in vitro and zebrafish model studies

Jehad Zuhair Tayyeb[1], Ajay Guru[2*], Karthikeyan Kandaswamy[2], Divya Jain[3], Chandrakumar Manivannan[4], Khairiyah Binti Mat[5,6*], Mohd Asif Shah[7,9,10*] and Jesu Arockiaraj[8*]

## Abstract

Wound infections resulting from pathogen infiltration pose a significant challenge in healthcare settings and everyday life. When the skin barrier is compromised due to injuries, surgeries, or chronic conditions, pathogens such as bacteria, fungi, and viruses can enter the body, leading to infections. These infections can range from mild to severe, causing discomfort, delayed healing, and, in some cases, life-threatening complications. Zinc oxide (ZnO) nanoparticles (NPs) have been widely recognized for their antimicrobial and wound healing properties, while cinnamic acid is known for its antioxidant and anti-inflammatory activities. Based on these properties, the combination of ZnO NPs with cinnamic acid (CA) was hypothesized to have enhanced efficacy in addressing wound infections and promoting healing. This study aimed to synthesize and evaluate the potential of ZnO-CN NPs as a multifunctional agent for wound treatment. ZnO-CN NPs were synthesized and characterized using key techniques to confirm their structure and composition. The antioxidant and anti-inflammatory potential of ZnO-CN NPs was evaluated through standard in vitro assays, demonstrating strong free radical scavenging and inhibition of protein denaturation. The antimicrobial activity of the nanoparticles was tested against common wound pathogens, revealing effective inhibition at a minimal concentration. A zebrafish wound healing model was employed to assess both the safety and therapeutic efficacy of the nanoparticles, showing no toxicity at tested concentrations and facilitating faster wound closure. Additionally, pro-inflammatory cytokine gene expression was analyzed to understand the role of ZnO-CN NPs in wound healing mechanisms. In conclusion, ZnO-CN NPs demonstrate potent antioxidant, anti-inflammatory, and antimicrobial properties, making them promising candidates for wound treatment. Given their multifunctional properties and non-toxicity at tested concentrations,

*Correspondence:
Ajay Guru
ajayguru.sdc@saveetha.com
Khairiyah Binti Mat
khairiyah@umk.edu.my
Mohd Asif Shah
m.asif@kardan.edu.af
Jesu Arockiaraj
jesuaroa@srmist.edu.in

Full list of author information is available at the end of the article

ZnO-CN NPs hold significant potential as a therapeutic agent for clinical wound management, warranting further investigation in human models.

**Keywords** Cinnamic acid, Zinc oxide nanoparticle, Wound healing, Nanomedicine, Zebrafish model, Wound infection

## Introduction

Wounds represent vulnerable points of entry for a variety of pathogens, each presenting unique challenges and complications upon infection. Among these, *Staphylococcus aureus*, a Gram-positive bacterium, stands out as a common culprit in wound infections. It possesses an array of virulence factors, including surface adhesins and toxins, facilitating its adherence to host tissues and evasion of immune defences [1]. Moreover, *S. aureus* can produce enzymes like coagulase and hyaluronidase, which contribute to tissue destruction and facilitate bacterial dissemination within the wound site [2]. *Escherichia coli*, a Gram-negative bacterium commonly found in the gastrointestinal tract, can also cause wound infections, particularly in cases of contaminated wounds or surgical site infections [3]. Certain strains of *E. coli*, such as those producing extended-spectrum beta-lactamases (ESBLs) or carbapenemases, pose significant challenges due to their resistance to multiple antibiotics [4]. *Pseudomonas aeruginosa*, another Gram-negative bacterium, is notorious for its ability to thrive in moist environments and cause opportunistic infections, particularly in immunocompromised individuals or those with chronic wounds [5]. *P. aeruginosa* secretes an arsenal of virulence factors, including exotoxins and enzymes, which contribute to tissue damage, inflammation, and resistance to host defences. Additionally, its ability to form biofilms enhances its persistence in wounds and complicates treatment [6]. *Vibrio vulnificus*, a halophilic Gram-negative bacterium commonly found in marine environments, poses a significant risk for wound infections, especially in individuals with open wounds exposed to contaminated seawater or seafood [7]. *V. vulnificus* secretes potent toxins and enzymes, leading to tissue necrosis and systemic complications such as septicemia, particularly in individuals with underlying liver disease or compromised immune function [8].

The utilization of cinnamic acid (CN) coated with zinc oxide nanoparticles (ZnO NPs) holds promising potential for the treatment and prevention of wound infections. It is anticipated that the antioxidant properties inherent in ZnO-CN NPs may effectively alleviate oxidative stress at the wound site [9]. Oxidative stress is a known hindrance to wound healing processes and can exacerbate tissue damage, thereby fostering an environment conducive to infection [10]. By scavenging free radicals and diminishing oxidative damage, it is foreseeable that these nanoparticles could foster a more conducive wound healing environment, thereby augmenting tissue repair and regeneration [11]. Moreover, it is predicted that the combined antimicrobial activity of ZnO NPs and CN could efficiently target a broad spectrum of wound-infecting pathogens. ZnO NPs have demonstrated antimicrobial efficacy against both Gram-positive and Gram-negative bacteria, fungi, and viruses [12]. The incorporation of CN is anticipated to further potentiate this antimicrobial activity, potentially through mechanisms such as disrupting bacterial cell membranes, inhibiting enzyme activity, or interfering with microbial signaling pathways. Additionally, the use of NPs presents unique advantages in wound care, including enhanced penetration into biofilms and deeper wound tissues, as well as sustained release of therapeutic agents.

Adult zebrafish also serve as valuable models for studying wound healing, offering unique advantages for investigating the process in a more mature organism [13]. Unlike zebrafish larvae, adult zebrafish possess fully developed immune systems, making them suitable for studying immune responses to injury and infection in a context more relevant to adult humans [14]. Additionally, adult zebrafish exhibit robust regenerative abilities, particularly in tissues such as the fins, heart, and spinal cord, allowing for the investigation of tissue regeneration mechanisms following injury [15]. Adult zebrafish can be subjected to various types of wounds, including fin amputation, tail fin transection, and skin puncture, enabling researchers to study different aspects of wound healing, including inflammation, wound closure, tissue regeneration, and scar formation [16, 17]. Furthermore, adult zebrafish are genetically tractable and amenable to experimental manipulations, such as pharmacological treatments, gene knockdowns, and transgenic approaches, facilitating the elucidation of molecular mechanisms underlying wound healing processes [15]. This research study aims to explore the synergistic potential of ZnO-CN NPs in targeting biofilm formation receptors of wound-infecting pathogens and modulating genes associated with wound healing processes. By harnessing the unique properties of ZnO-CN NPs, including their antimicrobial and antioxidant activities, we seek to enhance wound healing outcomes and mitigate the risk of infection. Through comprehensive analysis utilizing a zebrafish wound healing model, we aim to elucidate the mechanisms underlying the therapeutic efficacy of ZnO-CN NPs in promoting tissue repair and regeneration.

## Materials and methods

### Preparation of zinc oxide-cinnamic acid nanoparticles (ZnO-CN NPs)

ZnO-CN NPs are synthesized by first preparing a 0.1 M solution of zinc acetate dihydrate in deionized water (24.55 g in 100 ml) and a 0.1 M solution of sodium hydroxide in deionized water (4 g in 100 ml). Concurrently, a 1 mg/ml solution of CN is prepared to act as a reducing agent. The zinc acetate solution is then added dropwise to the sodium hydroxide solution with vigorous stirring. Upon heating, a white precipitate forms, indicating the formation of ZnO-CN NPs. The mixture is cooled, and the precipitate is collected by centrifugation. It is washed with ethanol and deionized water to remove impurities and then dried. The ZnO-CN NPs are characterized using several techniques. Scanning Electron Microscopy (SEM) analysis is performed by depositing a drop of the NPs suspension onto a silicon wafer, allowing it to dry, and then sputter-coating with gold before imaging (Carl Zeiss- Sigma 300, Germany). Fourier Transform Infrared Spectroscopy (FTIR) is conducted on a pellet of the NPs using an FTIR spectrometer (BRUKER ALPHA II, Germany). X-ray Diffraction (XRD) analysis is carried out using a powdered sample with a Bruker D8 Advance X-ray diffractometer. UV-Vis spectroscopy is employed by dispersing the NPs in ethanol and measuring the absorbance spectrum using a UV-Vis spectrophotometer [18].

### Invitro anti-inflammatory and antioxidant analysis

To evaluate the inhibition of albumin denaturation, prepare a stock solution of human serum albumin (HSA) by dissolving it in phosphate buffer (pH 7.4) to a concentration of 5 mg/ml. Concurrently, disperse the synthesized ZnO-CN NPs in a suitable solvent to obtain a desired concentration. Prepare test solutions of anti-inflammatory agents by diluting them in the buffer. In a series of test tubes, mix equal volumes of HSA solution, test compounds, and nanoparticle dispersion, and incubate them at a specific temperature (e.g., 37 °C) for a defined time (e.g., 1 h). Heat a separate set of HSA tubes at the same conditions as a positive control for denaturation. After incubation, cool the tubes and subject them to heat stress (e.g., heating at 70 °C for 20 min). Then, measure the absorbance of the samples at 660 nm using a UV-Vis spectrophotometer. The decrease in absorbance in the presence of the ZnO-CN NPs compared to the control indicates the inhibition of albumin denaturation, suggesting potential anti-inflammatory activity.

Prepare a reaction mixture consisting of a hydroxyl radical source, such as Fenton's reagent (typically 1:1 mixture of 10 mM $FeSO_4$ and 10 mM $H_2O_2$ solutions) The Fenton reaction involves the reaction of $H_2O_2$ with ferrous ions ($Fe^{2+}$) to produce hydroxyl radicals. Incubate the reaction mixture with ZnO-CN NPs at the room temperature. Add salicylic acid to initiate the reaction between hydroxyl radicals and salicylic acid, forming 2,3-dihydroxybenzoic acid. After incubation, stop the reaction by adding trichloroacetic acid (TCA) and then add thiobarbituric acid (TBA) to develop a pink chromogen. Heat the tubes, cool them, and centrifuge. Measure the absorbance of the supernatant at the wavelength of 532 nm using a UV-Vis spectrophotometer.

### Antimicrobial assays

Culture each pathogen of *S. aureus*, *E. coli*, *P. aeruginosa*, *and V. vulnificus* separately in appropriate growth media until reaching mid-log phase. Dilute the cultures to obtain a standardized bacterial suspension of about $5\times10^6$ CFU/mL. Then prepare a series of dilutions of the NPs stock solution in the respective growth media to cover a range of concentrations. In a 96-well microplate, dispense aliquots of the bacterial suspension into each well, followed by adding different concentrations of NPs. Amoxicillin and untreated was used as positive and control. Incubate the microplate at the appropriate temperature for each pathogen (e.g., 37 °C for *S. aureus* and *E. coli*, 42 °C for *V. vulnificus*, and 30 °C for *P. aeruginosa*) for 18–24 h. Following incubation, assess bacterial growth visually or by measuring optical density at a suitable wavelength using a microplate reader. The MIC is defined as the lowest concentration of treatment at which no visible growth or significant decrease in optical density is observed compared to the control.

In the well diffusion method, agar plates are prepared by pouring molten agar containing appropriate growth media for each pathogen, such as nutrient agar for *S. aureus* and *E. coli*, Mueller-Hinton agar for *P. aeruginosa*, and tryptic soy agar supplemented with 2% NaCl for *V. vulnificus*. After solidification, bacterial suspensions of $5\times10^6$ are spread evenly on the surface of the agar plates using a sterile swab. Wells are then created in the agar using a sterile cork borer. Different concentrations of the synthesized NPs solution are treatment into the well. Positive control (Amoxicillin) and control (untreated) are also included. The plates are then incubated at the room temperature. After incubation, the zones of inhibition around the NPs-treated wells is measured in millimeter (mm) using a calibrated ruler.

### Ligand and receptor interaction studies

The experimental procedure involved initial retrieval of crystal structures of receptors relevant to *S. aureus*, *E. coli*, *P. aeruginosa*, and *V. vulnificus* from the Protein Data Bank (https://www.rcsb.org/). PyMOL (https://pymol.org/) was utilized to prepare the receptor structures by removing water molecules and non-essential ligands. Cinnamic acid's 3D structure was obtained from

PubChem (https://pubchem.ncbi.nlm.nih.gov/) and converted into suitable formats using Open Babel GUI Ver 2.0. AutoDock VER 1.5.7 was employed for molecular docking studies to predict binding interactions between cinnamic acid and the receptors. Docking parameters were set, and binding affinity was evaluated by analyzing docking results, including binding energy and interaction patterns. Finally, Discovery Studio Visualizer software was used to visualize the 3D and 2D binding interactions between cinnamic acid and the receptor proteins [19].

## Invivo studies

### *Zebrafish toxicity*

Healthy adult wild-type zebrafish (*Danio rerio*) were obtained from Tarun Fish Farm (Chennai, India). The zebrafish were acclimatized in a controlled aquatic environment maintained at a temperature of 28 °C±1 °C, with a pH range of 7.0-7.5 and a 14:10 light-dark cycle. During acclimatization, the zebrafish were housed in 10 L glass tanks filled with dechlorinated water and provided with aeration and filtration systems [20]. Following a one-week acclimatization period to ensure physiological adjustment, the zebrafish were randomly divided into experimental groups, with each group consisting of 6 zebrafish individuals to ensure adequate statistical analysis. The experimental groups were exposed to ZnO-CN NPs of varying concentrations, ranging from 40 µg/mL to 80 µg/mL. Throughout the 1-week exposure period, zebrafish survival rate was monitored daily. Survival rate was calculated as the percentage of surviving zebrafish relative to the total number of zebrafish in each group at the initiation of the experiment [21].

### *Zebrafish wound closure experiments*

In the in vivo wound healing experiment, zebrafish ($n$=6/group) were distributed into four groups: a control, wounded zebrafish, and two experimental groups treated with Zn-CN NPs at concentrations of 40 µg/mL and 80 µg/mL, respectively. Fish were anesthetized via immersion in a solution of 0.2% Tricaine methanesulfonate before being wounded with a sterilized scalpel behind the gill region, closer to the zebrafish's lateral line. Every third day, Zn-CN NPs were treated to wounded zebrafish, and the healing process was monitored, with daily photographs taken. Zebrafish were anesthetized at specific intervals (0, 7, and 14-days post-injury), and the wounded sites were photographed and assessed for closure using Image J software. Wound healing progress was evaluated by periodically examining the wound area, with injured locations identified by discerning differences in skin color between affected and unaffected regions. Healing progression was tracked until the wounded area fully regenerated, returning to its original coloration, indicating completion of the healing process [13].

**Table 1** Primers used for gene expression

| Gene | Forward primer (5´-3´) | Reverse primer (5´-3´) | Accession number |
|---|---|---|---|
| *mmp13* | GAGAAGGTTTGGGCTCT CTATG | TGAGTTGCTGTCTT CCTTGTAG | AF506756 |
| *tnf-a* | AGAAGGAGAGTTGCCTTT ACCGCT | AACACCCTCCATAC ACCCGACTTT | AF025305 |
| *il-1β* | TCAAACCCCAATCCACA GAG | TCACTTCACGCTCT TGGATG | AY340959.1 |
| *β actin* | AATCTTGCGGTATCCACG AGACCA | TCTCCTTCTGCATC CTGTCAGCAA | AF025305 |

### *Histology analysis*

Zebrafish from different treatment groups were euthanized at specific time points post-injury, and the wounded areas were carefully dissected. Tissues were fixed in 4% paraformaldehyde solution, followed by dehydration through a series of ethanol washes and embedding in paraffin wax. Sections of approximately 5–10 µm thickness were obtained using a microtome and mounted onto glass slides. Hematoxylin and eosin (H&E) staining was performed to visualize tissue histology.

### *Gene expression studies*

Adult zebrafish were categorized into four groups: treatment 1 (ZnO-CN NPs at 40 µg/mL), treatment 2 (ZnO-CN NPs at 80 µg/mL), model (wounded zebrafish), and unwounded (control). Tissue samples from the wounded site were collected and stored at -80 °C. The pooled wound tissue underwent homogenization (Polytron PT 1200E, Kinematic, Switzerland) for RNA isolation using TRIzol reagent (Invitrogen, Carlsbad, CA, USA) [22]. RNA concentration was determined using a NanoDrop One, followed by cDNA synthesis with 2.5 µg of isolated RNA and a PrimeScript 1st strand cDNA synthesis kit (TaKaRa®, Tokyo, Japan) per manufacturer's instructions. Synthesized cDNA samples were diluted 30-fold with nuclease-free water and stored at -20 °C until further use. Primers used in this study was mentioned in Table 1. Zebrafish β-actin served as the housekeeping gene. Quantitative real-time PCR (qRT-PCR) was conducted using a Thermal Cycler Dice Real-Time System (TaKaRa®) following a previously published protocol with slight modifications. Briefly, each qRT-PCR reaction comprised 3 µl of cDNA template, 1 µl (10 µM) of each forward and reverse primer, and 5 µl TB Green Premix Ex Taq II (TaKaRa®) qPCR mix. Primer specificity was verified through a standard three-step thermal cycling profile with an annealing temperature of 56 °C, followed by a single dissociation reading step. Relative expression fold changes were calculated using the $2^{-\Delta\Delta CT}$ method [23].

### *Statistical analysis*

Statistical analyses were conducted using GraphPad prism software (Version 8, San Diego, CA, USA). Significance between control and treated group was assessed using one-way analysis of variance (ANOVA) followed by Tukey's post hoc test. A significance difference of $p<0.05$ was applied, and all data are expressed as mean ± standard deviation.

## Results

### Characterization of Zn-CN NPs

The characterization results indicate that the cinnamic acid and zinc oxide nanoparticles possess distinct structural and chemical properties. SEM reveals a rod-like morphology, suggesting the formation of elongated structures. This morphology could potentially enhance specific functionalities such as drug delivery or catalysis by providing a larger surface area. FTIR analysis identifies characteristic peaks at wave numbers 632.82, 706.17, 832.84, 1048.58, 1358.40, 1501.71, and 2350.65, indicating the presence of functional groups associated with both cinnamic acid and zinc oxide. These peaks correspond to various chemical bonds and molecular vibrations, providing insight into the composition and bonding within the nanoparticles. XRD analysis reveals that the nanoparticles exhibit a crystalline phase of approximately 30.1% and an amorphous phase of approximately 69.9%. The sharp peaks associated with cinnamic acid suggest a partially crystalline structure; however, when incorporated into the ZnO nanoparticle matrix, the intensity and position of these peaks may shift due to interactions between the organic compound and the nanoparticles. For ZnO nanoparticles, prominent diffraction peaks at 31.7°, 34.4°, 36.3°, 47.5°, and 56.6° correspond to the (100), (002), (101), (102), and (110) crystal planes, confirming the presence of a hexagonal wurtzite structure. This crystallinity indicates the presence of ordered atomic arrangements within the nanoparticles, which can influence their physical and chemical properties. Furthermore, UV spectroscopy displays a peak at 268 nm, suggesting the presence of electronic transitions within the NPs (Fig. 1A-D).

### Inhibition of albumin denaturation and free radical scavenging activity

The results of the study on Zn-CN NPs indicate promising properties in combating protein denaturation and oxidative stress. In the albumin denaturation experiment, Zn-CN NPs at the higher concentration of 80 µg/mL exhibited 63% activity, slightly lower than the positive control, diclofenac, which showed 72% activity. This suggests that Zn-CN NPs effectively prevent protein denaturation similar to diclofenac. Similarly, in the hydroxyl radical scavenging assay, Zn-CN NPs at 80 µg/mL demonstrated 69% activity, comparable to the positive control, trolox, which exhibited 75% activity (Fig. 2). This indicates that Zn-CN NPs possess significant antioxidant abilities, capable of neutralizing harmful hydroxyl radicals effectively. Overall, these findings suggest that Zn-CN NPs hold promise as therapeutic agents for addressing conditions associated with protein misfolding and oxidative damage.

### Inhibition of biofilm formation

The MIC experiment with Zn-CN NPs revealed their effectiveness against a range of pathogenic bacteria, such as *S. aureus*, *P. aeruginosa*, *E. coli*, and *V. vulnificus*. The MIC values remained consistent at 40 µg/mL for all tested bacteria, indicating that concentrations at or above this level significantly ($p<0.05$) inhibited their growth (Fig. 3). This underscores the broad-spectrum antimicrobial activity of Zn-CN NPs across both Gram-positive and Gram-negative bacteria.

Additionally, the zone of inhibition assay confirmed the antimicrobial potential of Zn-CN NPs. At 40 µg/mL, Zn-CN NPs displayed zones of inhibition ranging from 6, 4, 8, and 4 mm against *S. aureus*, *P. aeruginosa*, *E. coli*, and *V. vulnificus*. Increasing the concentration to 80 µg/mL resulted in larger zones of inhibition (7, 4, 11, and 5 mm), indicating a dose-dependent response. While the zones of inhibition were better compared to the positive control, amoxicillin (50 µg/mL), at 80 µg/mL of Zn-CN NPs, the antimicrobial activity notably improved, surpassing that of amoxicillin against all tested pathogens (Fig. 4).

### Binding interaction with pathogenic receptor

The docking studies between CN and wound-infecting bacterial pathogens revealed varying values of binding affinity. *E. coli* exhibited the highest affinity (-6.3 kcal/mol), indicating a strong potential for CN to combat E. coli infections. The amino acid interactions involving LEU, PRO, HIS, and TYR likely contribute to this strong binding. *S. aureus* followed with a slightly lower affinity (-5.5 kcal/mol), suggesting significant interaction and potential efficacy against this pathogen. *P. aeruginosa* and *V. vulnificus* showed lower affinities (-3.1 kcal/mol and −2.8 kcal/mol, respectively), indicating weaker interactions (Fig. 5; Table 2). These findings suggest that CN could be particularly effective against E. coli and potentially S. aureus infections, supported by the observed binding affinities and amino acid interactions.

### Survival rate analysis in zebrafish

The in vivo toxicity of ZnO-CN NPs was assessed through survival rate analysis in four groups: control (unwounded fish), wounded zebrafish, and wounded zebrafish treated with ZnO-CN NPs at 40 µg/mL and 80 µg/mL. Wounded zebrafish exhibited a decreased

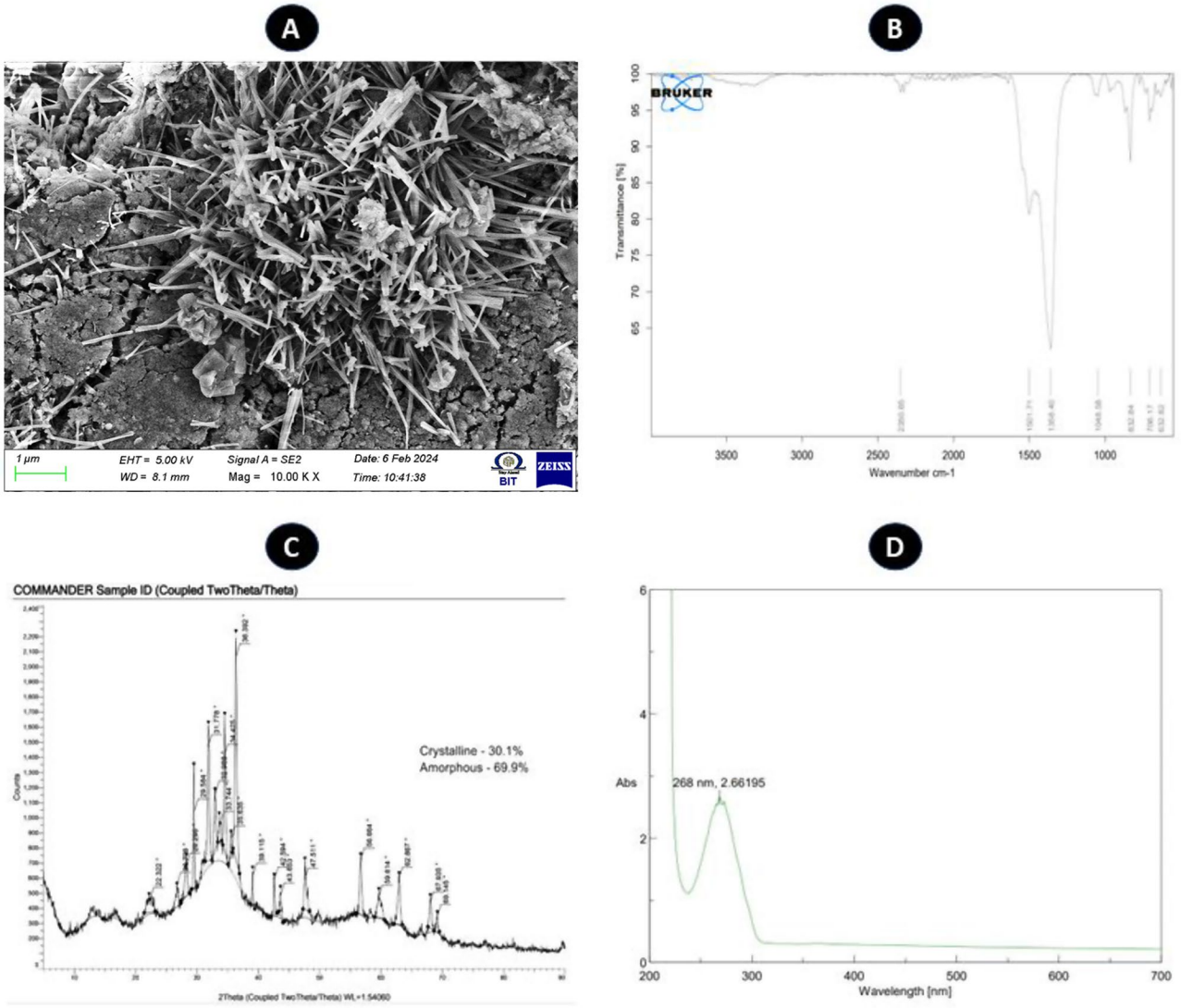


**Fig. 1** (**A**) SEM analysis of Zn-CN NPs revealing a rod-shaped morphology, (**B**) FTIR spectrum represent specific vibrational modes corresponding to functional groups, (**C**) XRD analysis of Zn-CN NPs illustrating the presence of a crystalline phase and amorphous phase, and (**D**) UV-Vis spectrum of synthesized Zn-CN NPs

survival rate (49%), indicating the adverse effects of injury alone. However, zebrafish treated with ZnO-CN NPs at both concentrations showed no significant reduction in survival compared to the control group, suggesting that the nanoparticles did not induce toxicity. These findings indicate that ZnO-CN NPs, at the tested concentrations, are non-toxic and well-tolerated by zebrafish (Fig. 6).

### Wound healing activity

The wound healing activity of ZnO-CN NPs was investigated on wounded zebrafish, focusing on concentrations of 40 µg/mL and 80 µg/mL over a period of 7 and 14 days post-wounding (dpw). Notably, treatment with ZnO-CN NPs at 40 µg/mL exhibited a 54% closure of wounds at 7 dpw, while at 80 µg/mL, the closure significantly ($p<0.05$) increased to 62%. Remarkably, by 14 dpw, the closure rates further improved to 70% and 93% for 40 µg/mL and 80 µg/mL concentrations when compared to the control group (Fig. 7). These findings underscore the potential efficacy of ZnO-CN NPs in promoting accelerated wound closure in zebrafish models, suggesting their promise for further exploration in wound healing applications.

### Histopathological studies

In this histology study, Zebrafish wounded tissue samples were analyzed after treatment with ZnO-CN NPs at concentrations of 40 µg/mL and 80 µg/mL. The tissue layers including skeletal muscle, dermal layer, granulation tissue, and epithelial layer with immune cell infiltration were examined before and after ZnO-CN NPs treatment in wounded zebrafish. Before treatment, the wounded zebrafish tissue displayed a lack of an epithelial layer,

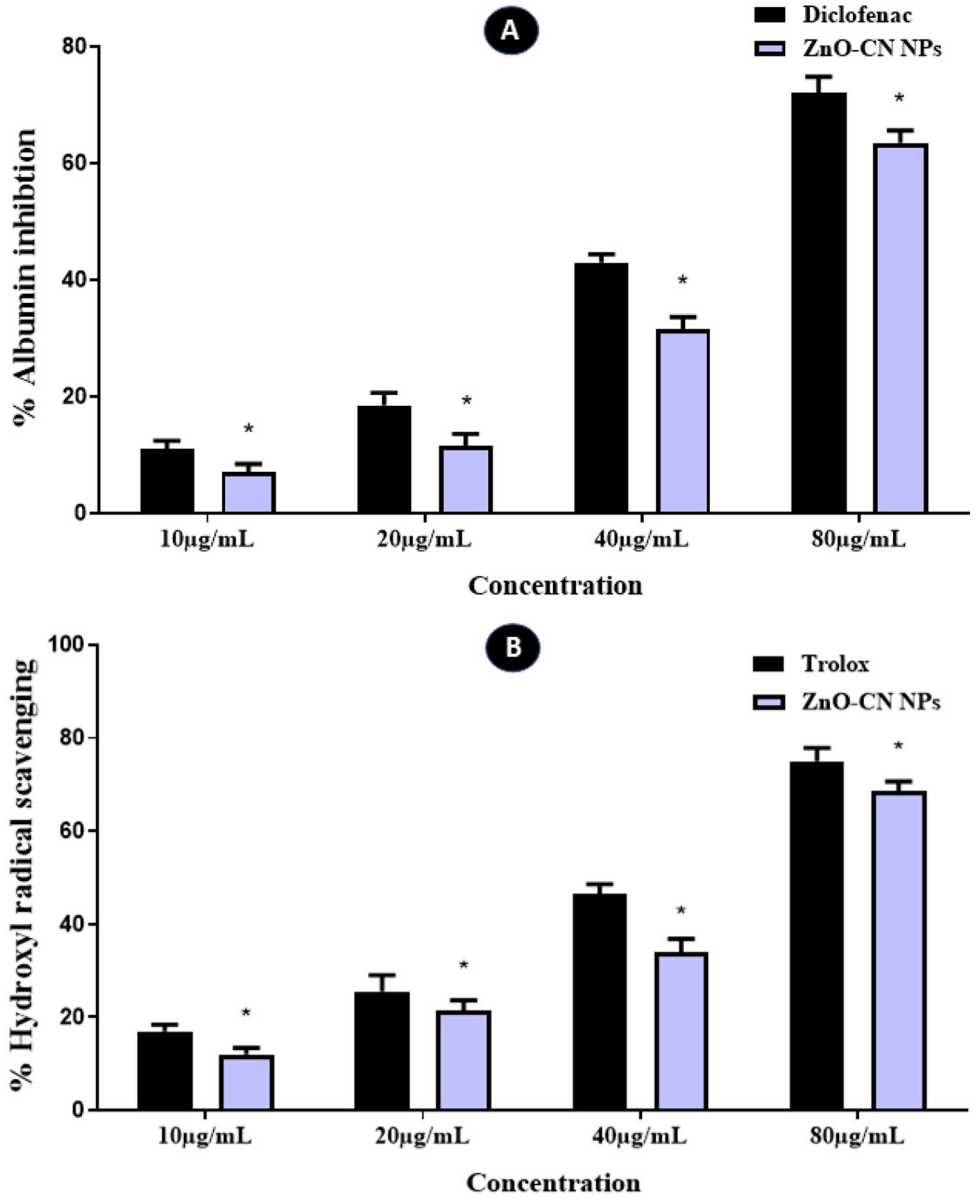


**Fig. 2** (**A**) Albumin denaturation Inhibition and (**B**) Hydroxyl radical scavenging activity of Zn-CN NPs at different concnetrations (10 µg/mL, 20 µg/mL, 40 µg/mL, and 80 µg/mL). Diclofenac and Trolox was used as a positive control. The * represented the level of significance ($p < 0.05$) when the results were compared to the control. Data were presented as mean ± SD of three independent experiments

indicating an impairment in the initial stages of wound healing. However, after treatment and examination after 14 days, the development of skeletal muscle, dermal layer, granulation tissue, and epithelial layer with immune cell infiltration was observed (Fig. 8). The results of the histology study indicate that the treatment of ZnO-CN NPs had a significant impact on the wound healing process in zebrafish.

#### Expression level of wound healing related genes

To understand the molecular mechanism of ZnO-CN NPs treatment in wound healing, the gene expression levels of matrix metalloproteinase 13 (*mmp13*) and pro-inflammatory cytokines such as *tnf-α* and *il-1β* were assessed. The higher concentration of ZnO-CN NPs at 80 µg/mL was chosen for further gene expression studies due to its observed superior activity and lower toxicity. This study demonstrated that the wound-administered group exhibited a significant upregulation in the gene expression of *mmp13* (3.5-fold), *tnf-α* (5.7-fold), and *il-1β* (4.6-fold) (Fig. 9). Meanwhile, the expression levels of *mmp13* (1.7-fold), *tnf-α* (3.4-fold), and *il-1β* (2.3-fold) were significantly downregulated in the ZnO-CN NPs treated group (80 µg/mL) compared to the control group.

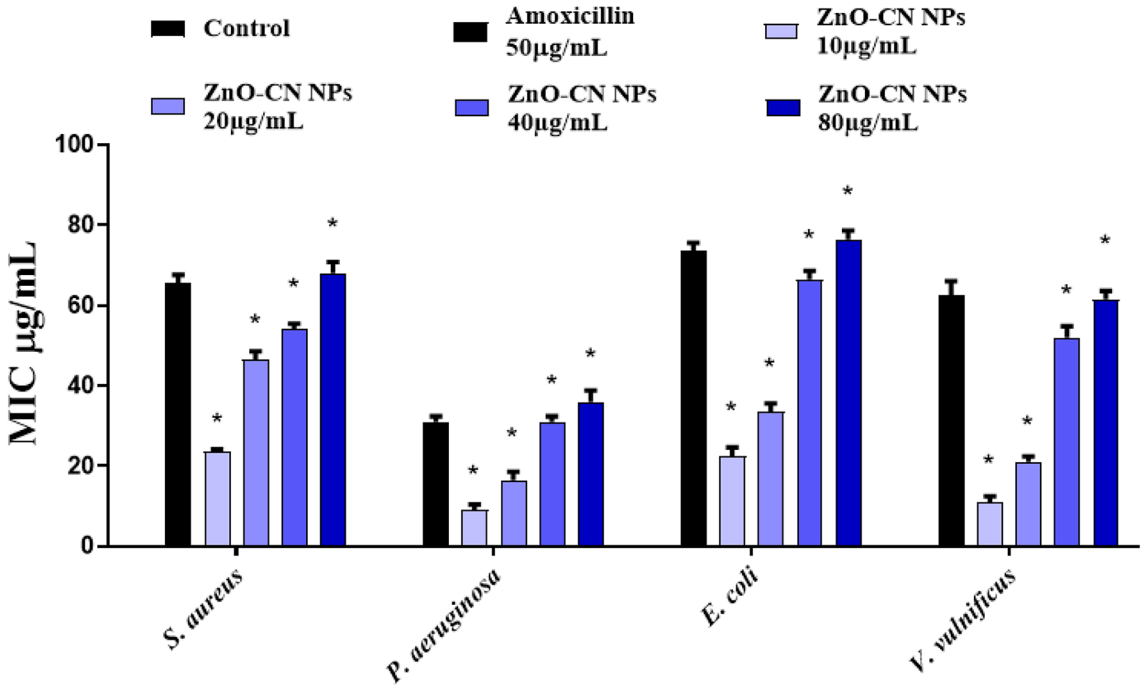


**Fig. 3** MIC of Zn-CN NPs at different concentration against dental pathogens of *S. aureus*, *P. aeruginosa*, *E. coli*, and *V. vulnificus*. Amoxicillin was used as positive control. The * represented the level of significance ($p < 0.05$) when the results were compared to the control. Data were presented as mean ± SD of three independent experiments

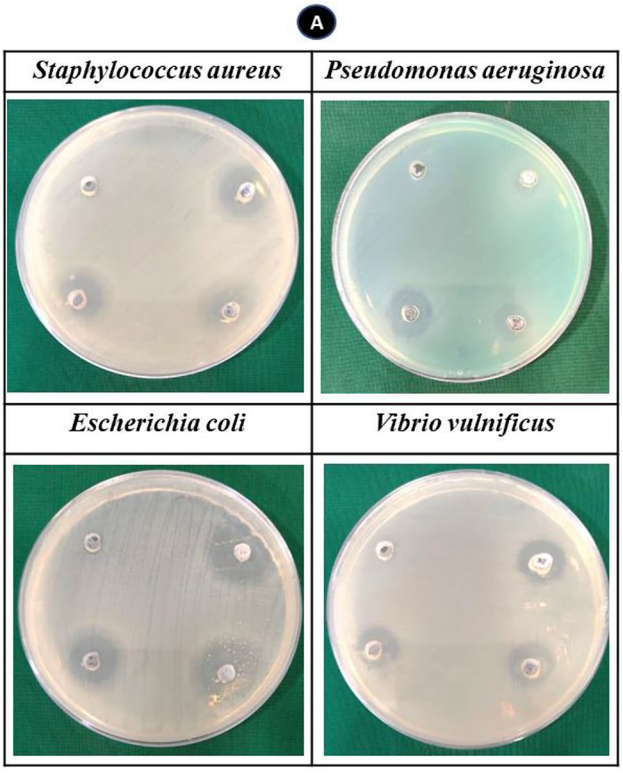


B

| Zone of Inhibition (mm) | | | | |
|---|---|---|---|---|
| Bacterial Strain | Control | Amoxicillin 50 µg/mL | ZnO-CN NPs 40 µg/mL | ZnO-CN NPs 80 µg/mL |
| *Staphylococcus aureus* | - | 7 | 6 | 7 |
| *Pseudomonas aeruginosa* | - | 2 | 4 | 4 |
| *Escherichia coli* | - | 10 | 8 | 11 |
| *Vibrio vulnificus* | - | 5 | 4 | 5 |

**Fig. 4** Zone of inhibition of different dental pathogen by Zn-CN NPs. (**A**). A – Control, B – Amoxicillin (50 µg/mL), C - Zn-CN NPs at 40 µg/mL, and D - Zn-CN NPs at 80 µg/mL. (**B**) Zone of inhibition measured at mm

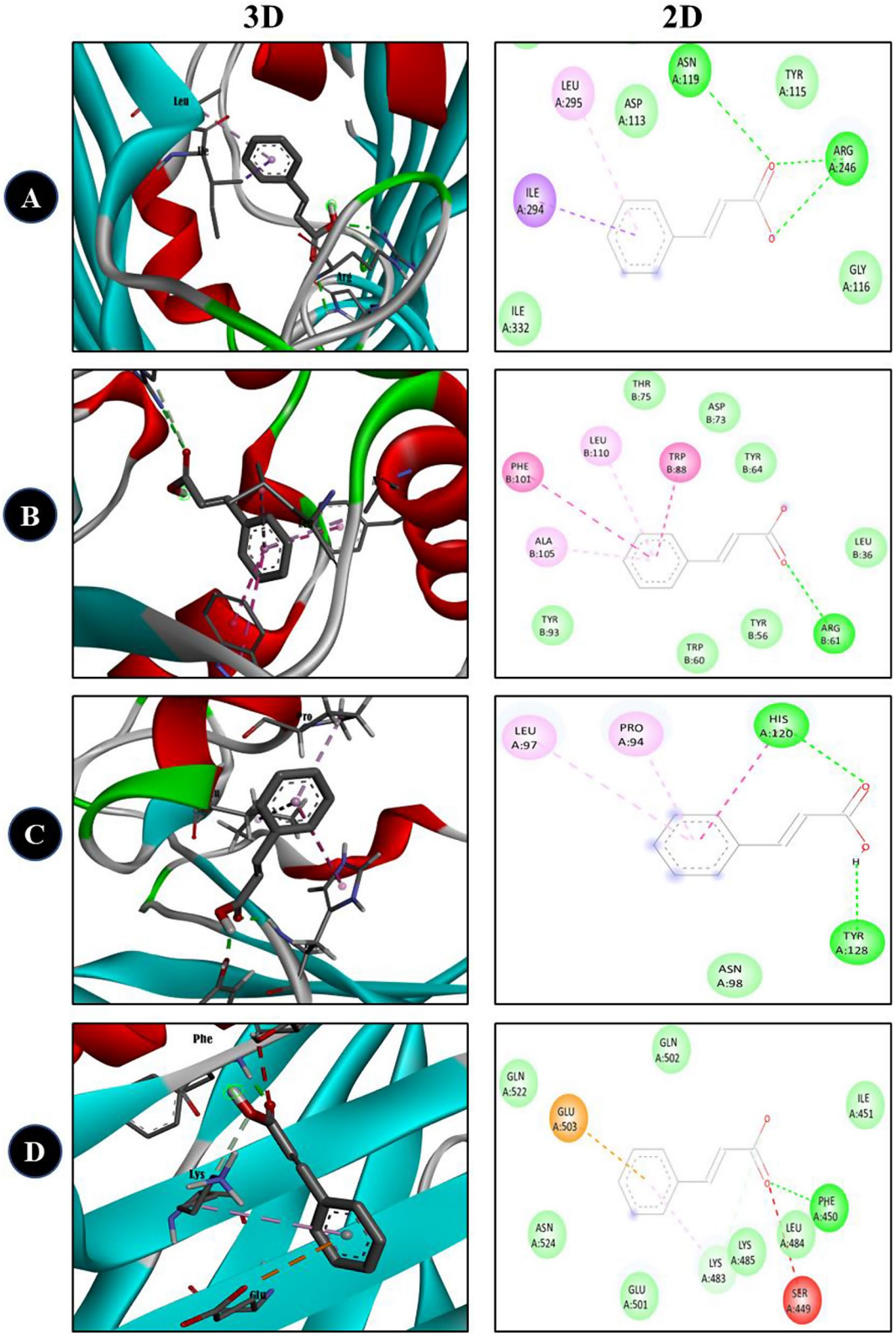


**Fig. 5** 3D and 2D interaction images of CN and wound-infecting bacterial pathogens. (**A**) Sortase A (**B**) LasR, (**C**) Outer membrane porin, (**D**) EpsD. The interaction is observed with amino acids such as PRO (Proline), PHE (Phenylalanine), TYR (Tyrosin), LYS (Lysine), ILE (Isoleucine), VAL (Valine), SER (Serine), TRP (Tryptophan), LEU (Leucine), HIS (Histidine), ARG (Arginine), ASN (Asparagine), ALA (Alanine) and GLU (Glutamic acid)

**Table 2** Amino acid and binding affinity value of the vanillic acid interaction with different dental pathogen receptors. PRO (proline), PHE (phenylalanine), TYR (Tyrosin), LYS (lysine), ILE (isoleucine), VAL (Valine), SER (serine), TRP (tryptophan), LEU (leucine), HIS (histidine), ARG (arginine), ASN (Asparagine), ALA (Alanine) and GLU (glutamic acid)

| | Receptor (PDB ID) | Ligand | Binding affinity (kcal/mol) | Amino acid interaction |
|---|---|---|---|---|
| 1. | *S. aureus*: Sortase A-substrate Complex (SrtA) **(**PDB: 2KID**)** | Cinnamic acid | -5.5 | ILE, LEU, ASN, ARG |
| 2. | *P. aeruginosa*: LasR (PDB: 4NG2) | Cinnamic acid | -3.1 | ALA, PHE, LEU, TRP, ARG |
| 3. | *E. coli*: Outer membrane porin (OmpC) (PDB: 2J1N) | Cinnamic acid | -6.3 | LEU, PRO, HIS, TYR |
| 4. | *V. vulnificus*: EpsD (PDB: 6I1Y) | Cinnamic acid | -2.8 | GLU, LYS, SER, PHE |

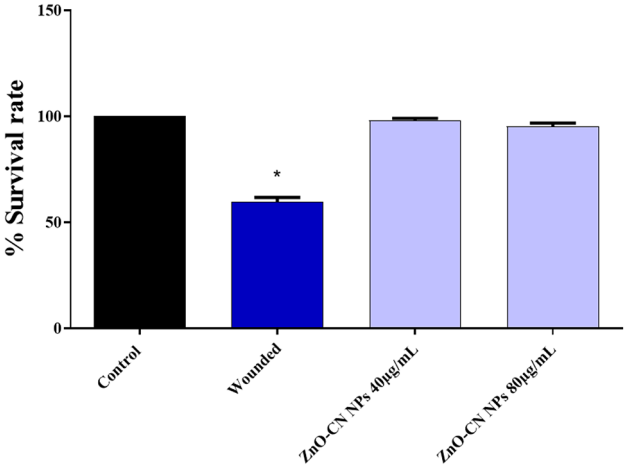


**Fig. 6** The survival rate analysis of zebrafish with different groups of control, wounded zebrafish, and exposure to ZnO-CN NPs (40 µg/mL and 80 µg/mL). The independent three experimental data were expressed as mean ± SD ($n = 6$/group). The significant difference at $p < 0.05$ was expressed as *

## Discussion

ZnO NPs have shown significant promise in wound healing due to their diverse biomedical properties [24–26]. In particular, the anti-inflammatory and antioxidant activities of ZnO NPs play a crucial role in enhancing wound healing processes [27]. For example, a study demonstrated that zinc oxide nanoparticles synthesized using *Strobilanthes cordifolia* leaf exhibited notable antioxidant, anti-cholinergic, anti-inflammatory, and wound healing activities, highlighting their potential therapeutic benefits [28]. CN, known for its antioxidant properties, is also beneficial in wound healing [9]. The coating of ZnO NPs with CN could potentially enhance these properties, offering a controlled release mechanism that prolongs the therapeutic effects at wound sites. The characterization of ZnO-CN NPs reveals crucial structural and chemical properties, essential for potential wound healing applications. In this study, the promising antioxidant and anti-inflammatory therapeutic potential of ZnO-CN NPs in wound healing can be attributed to their ability to stabilize proteins and scavenge harmful oxidative agents. The prevention of protein denaturation by these NPs helps maintain cellular integrity in the wound environment, reducing inflammation similarly to known anti-inflammatories like diclofenac. Their significant antioxidant activity also mitigates oxidative stress, a key impediment to the healing process, by neutralizing reactive oxygen species (ROS) that can damage tissue at the wound site. These functionalities not only accelerate the healing process but also enhance tissue repair. This result was supported by the previous studies that the *Aerva persica* mediated synthesis of ZnO NPs showed the dual therapeutic effect of antioxidant and anti-inflammatory property [29].

Antimicrobial activity is crucial for effective wound healing because it directly combats infection, one of the primary complications that can impede the healing process. Infections slow down healing by causing inflammation, increasing the burden of necrotic tissue, and disrupting new tissue formation [30]. Effective antimicrobial agents not only speed up the healing process by maintaining a cleaner wound environment but also minimizes the potential for developing antibiotic resistance, which is a significant concern with traditional antimicrobial treatments [31]. Moreover, preventing infections can decrease the likelihood of chronic wound conditions and systemic infections, leading to better overall outcomes in wound management. Recent studies have shown that electrospun membrane loaded with ZnO-NP exhibited the antibacterial activity against the *E. coli* and *S. aureus* [11]. Meanwhile in accordance with the previous result our study showed that the MIC and zone of inhibition assays collectively highlight the potent broad-spectrum antimicrobial activity of Zn-CN NPs, suggesting their significant utility in wound healing applications. This antimicrobial efficacy is critical in preventing and controlling infections at wound sites, particularly against common pathogens such as *S. aureus*, *P. aeruginosa*, *E. coli, and V. vulnificus*. The ability of ZnO-CN NPs to inhibit the growth of both Gram-positive and Gram-negative bacteria makes them an excellent candidate for topical wound dressings and coatings that require robust antimicrobial properties to ensure protection against a diverse array of pathogens. In the context of wound infections, the Sortase A-substrate complex (SrtA) in *S. aureus* is significant because it facilitates the attachment of surface proteins, including adhesins and toxins, to the bacterial cell wall. This attachment is essential for

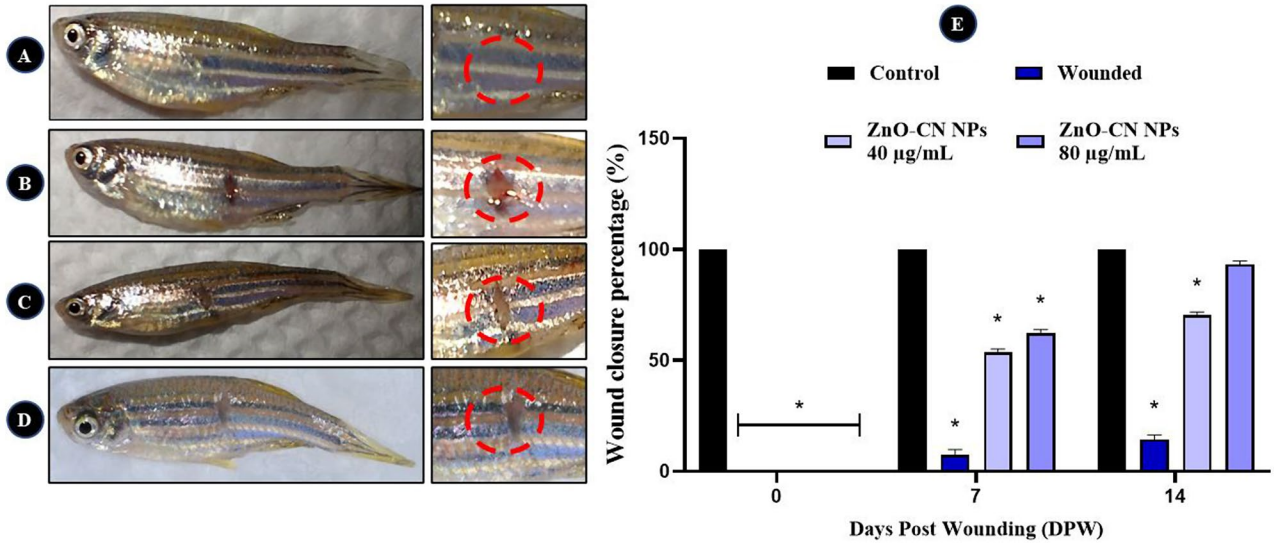


**Fig. 7** (**A**-**D**): Representative images of zebrafish wound healing under different treatment conditions. (**A**) Healthy control, (**B**) Wounded control, (**C**) Wounded zebrafish treated with ZnO-CN NPs at 40 µg/mL, and (**D**) Wounded zebrafish treated with ZnO-CN NPs at 80 µg/mL. (**E**) Graphical representation of wound closure measured using ImageJ software. Data are presented as mean ± SD from three independent experiments ($n = 6$/group). Statistical significance was determined with $p < 0.05$, indicated by *

*S. aureus* to adhere to and invade host tissues, initiating infection [32]. Adhesins help the bacteria to adhere to damaged tissues and host cells at the site of the wound, promoting colonization and biofilm formation, which can protect the bacteria from host defenses and antibiotics. Additionally, toxins that are anchored to the cell wall by SrtA can damage host cells and tissues, contributing to the pathogenesis of *S. aureus* infections [33]. One of the key virulence factors of *P. aeruginosa* in wound infections is the LasR protein, which is a transcriptional regulator that controls the expression of numerous virulence genes. *P. aeruginosa* is adept at forming biofilms, which are complex communities of bacteria encased in a matrix of extracellular polymeric substances [34]. LasR regulates the expression of genes involved in biofilm formation, promoting the attachment of *P. aeruginosa* to wound surfaces and protecting the bacteria from host immune defenses and antibiotics [35]. *E. coli* outer membrane that contributes to its virulence in wound infections is outer membrane porins (OmpC). OmpC allow the passage of small molecules, including nutrients and waste products, across the outer membrane [36]. In addition to nutrients, OmpC can also allow the passage of toxins and antibiotics into the bacterial cell. This can contribute to the pathogenicity of *E. coli* in wound infections by enabling the uptake of toxic substances produced by the host or by facilitating the entry of antibiotics, thereby promoting antibiotic resistance [37]. Virulence factor in *V. vulnificus* wound infections is the protein EpsD, which is involved in the biosynthesis of extracellular polysaccharides (EPS), a crucial component of the bacterial biofilm matrix. It has the ability to form biofilms on biotic and abiotic surfaces, including wounds [38]. Biofilms are complex communities of bacteria encased in a self-produced matrix of EPS, proteins, and DNA. This matrix provides structural support to the biofilm and protects bacteria from environmental stresses, including host immune responses and antibiotic treatments. EpsD is essential for the synthesis and secretion of EPS, which contributes to the formation and stability of *V. vulnificus* biofilms on wound surfaces [39]. In this study, CN, having shown significant binding affinity to essential bacterial proteins like Sortase A in *S. aureus*, LasR in *P. aeruginosa*, OmpC in *E. coli*, and EpsD in *V. vulnificus*, offered promising prospects for clinical application in preventing wound infections. These compounds could have served as lead molecules for novel antimicrobial therapeutics, complementing existing treatments or formulated into topical preparations and wound dressings for direct application to wounds. Through their ability to disrupt key virulence factors and inhibit biofilm formation, CN held potential for enhancing wound healing and reducing infection risk, particularly in high-risk populations or clinical settings where infection control was critical.

Wound healing is essential for restoring the structural and functional integrity of tissues, thereby promoting overall patient health and well-being [40]. Proper wound closure reduces the risk of infection, prevents further tissue damage, and facilitates the restoration of normal physiological function, allowing patients to resume their daily activities more quickly [41, 42]. Previous studies have investigated the wound healing activity of nanoemulsion with *Elaeis guineensis* leaf extract in zebrafish model. The effective wound closure process was observed

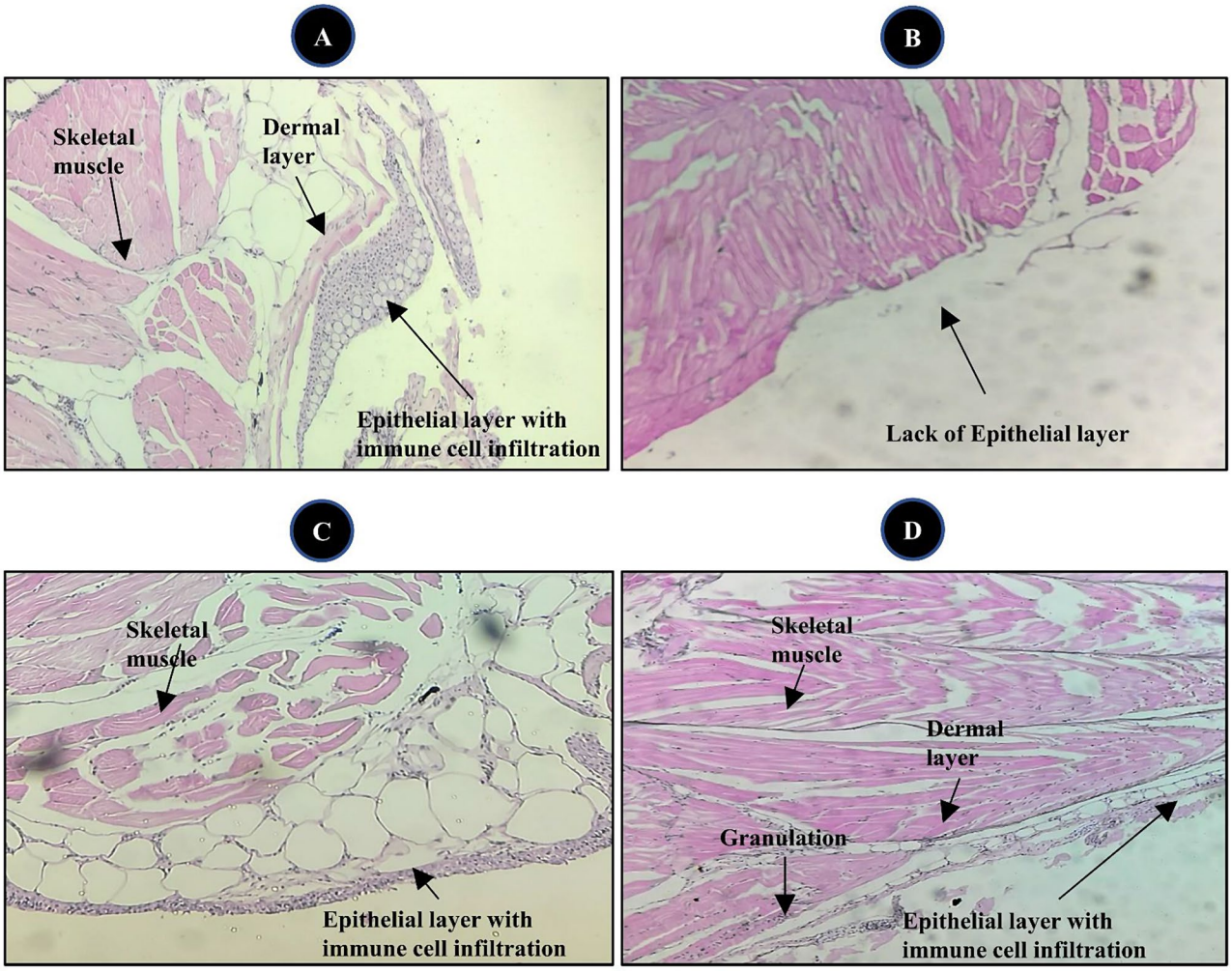


**Fig. 8** Histological analysis of wounded zebrafish tissue. (**A**) Healthy control, (**B**) Wound control (**C**) ZnO-CN NPs treatment at 40 µg/mL, and (**D**) ZnO-CN NPs treatment at 80 µg/mL. The tissue layers include skeletal muscle, dermal layer, granulation tissue, and epithelial layer with immune cell infiltration

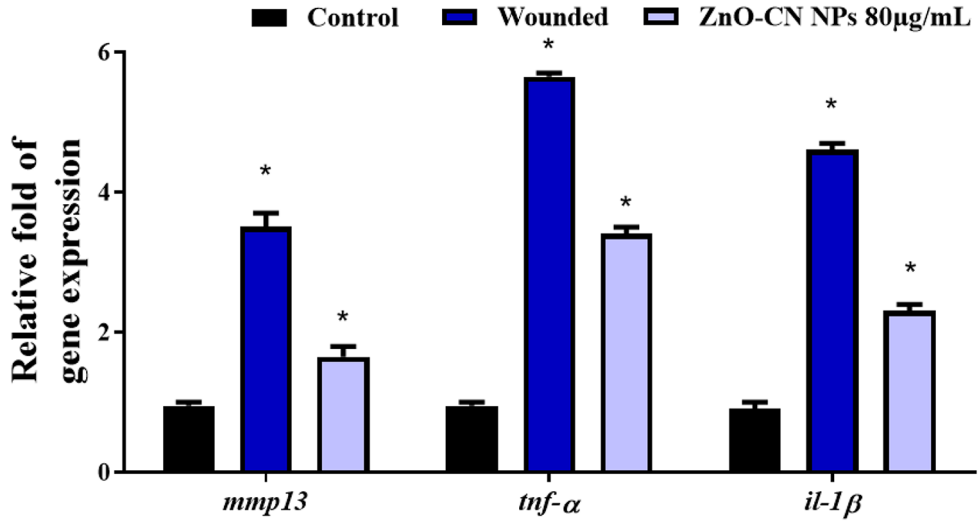


**Fig. 9** Effect of ZnO-CN NPs treatment group on the mRNA expression level of *mmp13*, *tnf-α*, *il-1β*. Data were expressed as mean + SD of three independent experiments. * $p < 0.05$ as compared to the control

after the treatment in zebrafish [13]. Similar studies of ZnO NPs coated with curcumin showed effective activity at 40 µg/mL and 80 µg/mL under in vitro conditions. Based on these findings, the selected concentrations of 40 µg/mL and 80 µg/mL were used for the ZnO-CN NPs in the in vivo studies. Similarly, the study's results regarding the toxicity analysis and wound healing activity of ZnO-CN NPs in zebrafish models present significant implications for potential applications in wound management. The absence of discernible toxicity in zebrafish, even at concentrations as high as 80 µg/mL, underscores the favorable safety profile of ZnO-CN NPs. This finding is particularly promising, as it suggests that these nanoparticles may be well-tolerated in biological systems, which is a crucial consideration for any therapeutic intervention. Additionally, the remarkable wound healing activity observed with ZnO-CN NPs highlights their potential as effective wound healing agents. Concentrations of 40 µg/mL and 80 µg/mL demonstrated accelerated closure of wounds compared to the control group, with the higher concentration showing particularly notable results, reaching a closure rate of 93% by 14 days post-wounding. Furthermore, the tissue repair during the wound healing process was confirmed through the histology experiment with the development of skeletal muscle, dermal layer, granulation tissue, and epithelial layer with immune cell infiltration. This accelerated wound closure suggests that ZnO-CN NPs have the ability to promote tissue regeneration and repair, potentially enhancing the overall wound healing process. These findings open up exciting possibilities for the development of ZnO-CN NPs-based wound dressings or topical formulations for clinical use. Incorporating ZnO-CN NPs into wound care products could offer a safe and effective approach to promote faster wound closure and improve patient outcomes. During wound healing, *mmp13* and pro-inflammatory cytokines *tnf-α* and *il-1β* plays a major role. The *mmp13* facilitates tissue remodelling by degrading extracellular matrix components, while pro-inflammatory cytokines like *tnf-α* and *il-1β* initiate and amplify the inflammatory response crucial for wound healing [43]. The *mmp13* activity promotes the breakdown of damaged tissue and the migration of inflammatory cells to the wound site, aiding in tissue repair [44]. The *tnf-α* and *il-1β* induce the expression of adhesion molecules and chemokines, recruiting leukocytes and amplifying the inflammatory cascade. Additionally, *il-1β* stimulates fibroblast proliferation and collagen synthesis, promoting tissue repair [45–47]. Together, these molecules play vital roles in orchestrating the various phases of wound healing, from inflammation to tissue remodelling. According to the earlier report, during the wound healing process, the downregulation of *mmp13*, *tnf-α* and *il-1β* was observed in the zebrafish model. In accordance with this report, in our study, the upregulation of these genes in the wound-administered group indicates an active inflammatory phase necessary for initiating the healing process. However, the downregulation of these genes in the ZnO-CN NPs treated group suggests a modulation of the inflammatory response, possibly leading to a more controlled and efficient healing process. These findings highlight the therapeutic potential of ZnO-CN NPs in wound management by regulating inflammatory signaling pathways and promoting tissue repair. As a future direction, we plan to extend this research to higher animal models to further evaluate the therapeutic potential of ZnO-CN NPs in wound healing. This approach will provide more robust and comprehensive data on the efficacy, biocompatibility, and long-term impact of ZnO-CN NPs in a more physiologically relevant context. Conducting studies in higher animal models will also allow for a deeper investigation into the molecular mechanisms underlying their modulation of the inflammatory response and tissue repair processes. Ultimately, this research aims to pave the way for clinical translation of ZnO-CN NPs as a promising therapeutic strategy in wound management and tissue regeneration.

## Conclusion

In conclusion, this study elucidates the multifaceted therapeutic potential of Zinc oxide-Cinnamic acid Nanoparticles (ZnO-CN NPs) in wound management. The synergistic combination of ZnO NPs and cinnamic acid (CN) offers a promising platform for enhancing wound healing through various mechanisms. The antioxidant and anti-inflammatory properties of ZnO NPs, coupled with the known benefits of CN in wound healing, create a potent formulation with the potential to modulate inflammatory responses and promote tissue repair. However, it is essential to highlight the potential toxicity of ZnO NPs. While they exhibit beneficial properties in wound healing, at higher concentrations or prolonged exposure, they may generate reactive oxygen species (ROS), leading to oxidative stress and cytotoxicity in surrounding healthy tissues. Thus, careful control of dosage, application frequency, and nanoparticle size is critical to minimize potential side effects. In addition, the widespread use of ZnO NPs in daily wound management presents certain challenges. The scalability of production, cost-effectiveness, and ensuring consistent biocompatibility and safety standards remain significant hurdles. Future research must focus on addressing these challenges, alongside conducting preclinical studies in animal models and clinical trials in human subjects to thoroughly evaluate the efficacy, safety, and long-term effects of ZnO-CN NPs. This will ultimately pave the way for their potential integration into routine clinical practice and commercial wound care products.

**Acknowledgements**
This research was supported under postdoctoral scheme publication under University Malaysia Kelantan.

**Author contributions**
J.Z.T, A.G, K.K, D.J, and C.M. wrote the main manuscript text. K.B.M, M.A.S and J.A. prepared figures and tables. All authors reviewed the manuscript.

**Data availability**
The data are available from the corresponding author upon reasonable request.

## Declarations

**Ethics approval**
All in vivo experiments adhered to the guidelines and regulations set forth by the Institutional Animal Ethics Committee (IAEC) of Saveetha Dental College, Chennai, India, under approval number BRULAC/SDCH/SIMATS/IAEC/06-2023/15. No permission was required for collecting the samples in these studies.

**Consent to participate**
No permission was required for collecting the samples in these studies and it is not applicable.

**Consent for publication**
Not applicable.

**Competing interests**
The authors declare no competing interests.

**Author details**
[1]Division of Clinical Biochemistry, Department of Basic Medical Sciences, College of Medicine, University of Jeddah, Jeddah 23890, Saudi Arabia
[2]Department of Cariology, Saveetha Dental College and Hospitals, Saveetha Institute of Medical and Technical Sciences, Saveetha University, Chennai, India
[3]Department of Microbiology, School of Applied & Life Sciences, Uttaranchal University, Dehradun, Uttarakhand 248007, India
[4]Division of Chemistry, Faculty of Engineering and Technology, SRM Institute of Science and Technology, Tiruchirapalli, India
[5]Department of Agricultural Sciences, Faculty of Agro-Based Industry, Universiti Malaysia Kelantan, Jeli Campus, Jeli 17600, Malaysia
[6]Advanced Livestock and Aquaculture Research Group, Faculty of Agro-Based Industry, Universiti Malaysia Kelantan, Jeli Campus, Jeli 17600, Malaysia
[7]Department of Economics, Kardan University, Parwane Du, Kabul 1001, Afghanistan
[8]Toxicology and Pharmacology Laboratory, Department of Biotechnology, Faculty of Science and Humanities, SRM Institute of Science and Technology, Kattankulathur, Chengalpattu District, Tamil Nadu 603203, India
[9]Division of Research and Development, Lovely Professional University, Phagwara144001, Punjab, India
[10]Centre of Research Impact and Outcome, Chitkara University Institute of Engineering and Technology, Chitkara University, Rajpura, Punjab140401, India

Received: 3 July 2024 / Accepted: 1 October 2024
Published online: 10 October 2024

**References**

1. Makeri D, Odoki M, Eilu E, Agwu E. Update on prevalence and antimicrobial resistance of Staphylococcus aureus and Pseudomonas aeruginosa isolated from diabetic foot ulcers in Africa: a systematic review and meta-analysis. Bull Natl Res Cent. 2023;47:145.
2. Tam K, Torres VJ. Staphylococcus aureus secreted toxins and extracellular enzymes. Microbiol Spectr. 2019;7.
3. Mundhada A, Tenpe S. A study of organisms causing surgical site infections and their antimicrobial susceptibility in a tertiary care Government Hospital. Indian J Pathol Microbiol. 2015;58:195.
4. Kizilates F, Yakupogullari Y, Berk H, Oztoprak N, Otlu B. Risk factors for fecal carriage of extended-spectrum beta-lactamase-producing and carbapenem-resistant Escherichia coli and Klebsiella pneumoniae strains among patients at hospital admission. Am J Infect Control. 2021;49:333–9.
5. Bobrov AG, Getnet D, Swierczewski B, Jacobs A, Medina-Rojas M, Tyner S, et al. Evaluation of Pseudomonas aeruginosa pathogenesis and therapeutics in military-relevant animal infection models. APMIS. 2022;130:436–57.
6. Chadha J, Harjai K, Chhibber S. Revisiting the virulence hallmarks of Pseudomonas aeruginosa a chronicle through the perspective of quorum sensing. Environ Microbiol. 2022;24:2630–56.
7. Yamazaki K, Kashimoto T, Kado T, Yoshioka K, Ueno S. Increased vascular permeability due to Spread and Invasion of Vibrio vulnificus in the wound infection exacerbates potentially fatal Necrotizing Disease. Front Microbiol. 2022;13.
8. Hu P, Liu G, Xu H, Su Y. Finger necrotizing fasciitis and Septicemia caused by Vibrio vulnificus. Surg Infect (Larchmt). 2024. https://doi.org/10.1089/sur.2023.284.
9. Ravikumar OV, Marunganathan V, Kumar MSK, Mohan M, Shaik MR, Shaik B, et al. Zinc oxide nanoparticles functionalized with cinnamic acid for targeting dental pathogens receptor and modulating apoptotic genes in human oral epidermal carcinoma KB cells. Mol Biol Rep. 2024;51:352.
10. Qiu X, Wu Y, Zhang D, Zhang H, Yu A, Li Z. Roles of oxidative stress and Raftlin in Wound Healing under negative-pressure wound therapy. Clin Cosmet Investig Dermatol. 2021;14:1745–53.
11. Khan A, ur R, Huang K, Jinzhong Z, Zhu T, Morsi Y, Aldalbahi A, et al. Exploration of the antibacterial and wound healing potential of a PLGA/silk fibroin based Electrospun membrane loaded with zinc oxide nanoparticles. J Mater Chem B. 2021;9:1452–65.
12. El-Fallal AA, Elfayoumy RA, El-Zahed MM. Antibacterial activity of biosynthesized zinc oxide nanoparticles using Kombucha extract. SN Appl Sci. 2023;5:332.
13. Zain MSC, Edirisinghe SL, Kim CH, De Zoysa M, Shaari K. Nanoemulsion of flavonoid-enriched oil palm (Elaeis guineensis Jacq.) Leaf extract enhances wound healing in zebrafish. Phytomedicine Plus. 2021;1.
14. Martins RR, Ellis PS, MacDonald RB, Richardson RJ, Henriques CM. Resident Immunity in tissue repair and maintenance: the zebrafish model coming of Age. Front Cell Dev Biol. 2019;7.
15. Naomi R, Bahari H, Yazid MD, Embong H, Othman F. Zebrafish as a Model System to study the mechanism of Cutaneous Wound Healing and Drug Discovery: advantages and challenges. Pharmaceuticals. 2021;14:1058.
16. Petrie TA, Strand NS, Tsung-Yang C, Rabinowitz JS, Moon RT. Macrophages modulate adult zebrafish tail fin regeneration. Development. 2014;141:2581–91.
17. Audira G, Suryanto ME, Chen KH-C, Vasquez RD, Roldan MJM, Yang C-C, et al. Acute and Chronic effects of Fin Amputation on Behavior performance of adult zebrafish in 3D locomotion test assessed with Fractal Dimension and Entropy analyses and their relationship to Fin Regeneration. Biology (Basel). 2022;11:969.
18. Rani P, Jenifer H, Prabhu A, David D, Devanesan S, AlSalhi MS et al. Enhancing anticancer efficacy: xovoltib-loaded chitosan-tripolyphosphate nanoparticles for targeted drug delivery against MCF-7 breast cancer cells. Mater Technol. 2024;39.
19. Balakrishnan D, Pragathiswaran C, Thanikasalam K, Mohanta YK, Saravanan M, Abdellattif MH. Molecular Docking and in Vitro Inhibitory Effect of Polyaniline (PANI)/ZnO nanocomposite on the growth of Struvite Crystal: a step towards control of UTI. Appl Biochem Biotechnol. 2022;194:4462–76.
20. Singh M, Guru A, Sudhakaran G, Pachaiappan R, Mahboob S, Juliet A, et al. Copper sulfate induced toxicological impact on in-vivo zebrafish larval model protected due to acacetin via anti-inflammatory and glutathione redox mechanism comparative biochemistry and physiology, part C copper sulfate induced toxicological impact on i. Comp Biochem Physiol Part C. 2022;262:109463.
21. Surya M, Sampath S, Vairamuthu SB, Sravanthy PG, Ramachandran B, Al-Ansari MM et al. Aloe vera - mediated silver-selenium doped fucoidan nanocomposites synthesis and their multi-faceted biological evaluation of antimicrobial, antioxidant and cytotoxicity activity. Mater Technol. 2024;39.
22. Guru A, Sudhakaran G, Velayutham M, Murugan R, Pachaiappan R, Mothana RA et al. Daidzein normalized gentamicin-induced nephrotoxicity and associated pro-inflammatory cytokines in MDCK and zebrafish: possible

mechanism of nephroprotection. Comp Biochem Physiol Part - C Toxicol Pharmacol. 2022;258 May:109364.
23. Livak KJ, Schmittgen TD. Analysis of relative gene expression data using real-time quantitative PCR and the 2-ΔΔCT method. Methods. 2001;25:402–8.
24. Singh AV, Gemmati D, Kanase A, Pandey I, Misra V, Kishore V et al. Nanobiomaterials for vascular biology and wound management: a review. Veins Lymphat. 2018;7.
25. Dwivedi C, Pandey I, Pandey H, Patil S, Mishra SB, Pandey AC, et al. In vivo diabetic wound healing with nanofibrous scaffolds modified with gentamicin and recombinant human epidermal growth factor. J Biomed Mater Res Part A. 2018;106:641–51.
26. Dwivedi C, Pandey I, Pandey H, Ramteke PW, Pandey AC, Mishra SB, et al. Electrospun Nanofibrous Scaffold as a potential carrier of Antimicrobial therapeutics for Diabetic Wound Healing and tissue regeneration. Nano- and Microscale Drug Delivery systems. Elsevier; 2017. pp. 147–64.
27. Le VAT, Trinh TX, Chien PN, Giang NN, Zhang X-R, Nam S-Y, et al. Evaluation of the performance of a ZnO-Nanoparticle-coated Hydrocolloid Patch in Wound Healing. Polym (Basel). 2022;14:919.
28. Kirubakaran D, Selvam K, Subramanian Shivakumar M, Rajkumar M, Kannan S, Navina B. Bio-fabrication of zinc oxide nanoparticles using Strobilanthes cordifolia: characterization and evaluation of antioxidant, anti-cholinergic, anti-inflammatory and wound healing activities. ChemistrySelect. 2024;9.
29. Fatima K, Asif M, Farooq U, Gilani SJ, Bin Jumah MN, Ahmed MM. Antioxidant and anti-inflammatory applications of Aerva Persica Aqueous-Root extract-mediated synthesis of ZnO nanoparticles. ACS Omega. 2024;9:15882–92.
30. Pino P, Bosco F, Mollea C, Onida B. Antimicrobial Nano-Zinc Oxide biocomposites for Wound Healing applications: a review. Pharmaceutics. 2023;15:970.
31. Shariati A, Moradabadi A, Azimi T, Ghaznavi-Rad E. Wound healing properties and antimicrobial activity of platelet-derived biomaterials. Sci Rep. 2020;10:1032.
32. Susmitha A, Bajaj H, Madhavan Nampoothiri K. The divergent roles of sortase in the biology of Gram-positive bacteria. Cell Surf. 2021;7:100055.
33. Motta C, Pellegrini A, Camaione S, Geoghegan J, Speziale P, Barbieri G, et al. Von Willebrand factor-binding protein (vWbp)-activated factor XIII and transglutaminase 2 (TG2) promote cross-linking between FnBPA from Staphylococcus aureus and fibrinogen. Sci Rep. 2023;13:11683.
34. Vanderwoude J, Fleming D, Azimi S, Trivedi U, Rumbaugh KP, Diggle SP. The evolution of virulence in Pseudomonas aeruginosa during chronic wound infection. Proc R Soc B Biol Sci. 2020;287:20202272.
35. Vetrivel A, Ramasamy M, Vetrivel P, Natchimuthu S, Arunachalam S, Kim G-S, et al. Pseudomonas aeruginosa Biofilm Formation Its Control Biol. 2021;1:312–36.
36. Ballén V, Cepas V, Ratia C, Gabasa Y, Soto SM. Clinical Escherichia coli: from Biofilm formation to New Antibiofilm Strategies. Microorganisms. 2022;10:1103.
37. Zhong Z, Emond-Rheault J-G, Bhandare S, Lévesque R, Goodridge L. Bacteriophage-Induced Lipopolysaccharide mutations in Escherichia coli lead to hypersensitivity to Food Grade surfactant Sodium Dodecyl Sulfate. Antibiotics. 2020;9:552.
38. Sartelli M, Coccolini F, Kluger Y, Agastra E, Abu-Zidan FM, Abbas AES, et al. WSES/GAIS/WSIS/SIS-E/AAST global clinical pathways for patients with skin and soft tissue infections. World J Emerg Surg. 2022;17:3.
39. Lee H, Im H, Hwang S-H, Ko D, Choi SH. Two novel genes identified by large-scale transcriptomic analysis are essential for biofilm and rugose colony development of Vibrio vulnificus. PLOS Pathog. 2023;19:e1011064.
40. Gaur S, Singhal S, Gaur S, Mishra R, Pandey I, Bajpai S. Mesalazine based topical hydrogel formulation enhances anti-oxidant and cytokine activity in wounded STZ-induced mice. J Drug Deliv Ther. 2022;12:51–7.
41. Falcone M, De Angelis B, Pea F, Scalise A, Stefani S, Tasinato R, et al. Challenges in the management of chronic wound infections. J Glob Antimicrob Resist. 2021;26:140–7.
42. Tiwari Pandey A, Pandey I, Kanase A, Verma A, Garcia-Canibano B, Dakua S, et al. Validating anti-infective activity of Pleurotus Opuntiae via standardization of its bioactive mycoconstituents through multimodal biochemical Approach. Coatings. 2021;11:484.
43. Lu J, Feng X, Zhang H, Wei Y, Yang Y, Tian Y, et al. Maresin-1 suppresses IL-1β-induced MMP-13 secretion by activating the PI3K/AKT pathway and inhibiting the NF-κB pathway in synovioblasts of an osteoarthritis rat model with treadmill exercise. Connect Tissue Res. 2021;62:508–18.
44. Toriseva M, Laato M, Carpén O, Ruohonen ST, Savontaus E, Inada M, et al. MMP-13 regulates growth of Wound Granulation tissue and modulates gene expression signatures involved in inflammation, Proteolysis, and cell viability. PLoS ONE. 2012;7:e42596.
45. Sheikh S, Rahman M, Gale Z, Luu NT, Stone PCW, Matharu NM, et al. Differing mechanisms of leukocyte recruitment and sensitivity to conditioning by shear stress for endothelial cells treated with tumour necrosis factor- α or interleukin-1 β. Br J Pharmacol. 2005;145:1052–61.
46. Chen X, Zhao M, Xie Q, Zhou S, Zhong X, Zheng J, Liao Y. Click-hydrogel delivered aggregation-induced emissive nanovesicles for simultaneous remodeling and antibiosis of deep burn wounds. Aggregate. 2024;5(1):e406. https://doi.org/10.1002/agt2.406
47. Zhao M, Kang M, Wang J, Yang R, Zhong X, Xie Q, Liao Y Stem Cell-Derived Nanovesicles Embedded in Dual-Layered Hydrogel for Programmed ROS Regulation and Comprehensive Tissue Regeneration in Burn Wound Healing. Adv Mater. 2024;36(32):2401369. https://doi.org/10.1002/adma.202401369

## Publisher's note